

Theoretical Analysis about Radial Electric Field in Toroidal Helical Systems

TODA Shinichiro* and ITOH Kimitaka

National Institute for Fusion Science, Oroshi-cho 322-6, Toki 509-5292, Japan

(Received: 5 December 2000 / Accepted: 27 August 2001)

Abstract

A set of the transport equations is analyzed, including the bifurcation of the radial electric field in toroidal helical systems. A hard transition is found in the profile of the radial electric field. The region where the electron root and ion root co-exist is obtained. The various types of the electrostatic-potential structures are found.

Keywords:

radial electric field, neoclassical transport, anomalous transport, transport barrier, turbulence suppression

1. Introduction

Recently, the internal transport barrier has been found in the ECRH plasma in CHS device. [1,2] The various types of the potentials have been obtained. The interface of domains with different electric field polarity has been pointed out theoretically for helical plasmas. [3] The internal transport barrier in heliotron plasmas, which is induced due to the electric field bifurcation, was theoretically studied based on the zero-dimensional model. [4,5] To study the interface of neighboring domains with different electric polarity, the one-dimensional transport analysis is needed. The investigation about the dynamics and the spatial structure of the transport barrier is extended to the one-dimensional model in order to compare with the experimental result. The possibility for the transport barriers (the edge transport barrier and the internal transport barrier) has been discussed based on the bifurcation model of the electric field; We have examined a set of one-dimensional transport equations which constitute the temporal evolution of the temperature and the diffusion equation the radial electric field in a slab plasma. [6] In this article, we examine the four (one-dimensional) transport equations which

describe the temporal evolutions of the density, the electron and ion temperatures, and the radial electric field in a cylindrical configuration. A numerical formula [7] for the non-axisymmetric part of the neoclassical flux is adapted. The electric field domain is studied in helical plasmas. We use the machine parameter for CHS device [8] when we solve the set of the transport equations. We study the radial profile of the electric field and examine the states which are related to the internal transport barrier. We also show the condition for the hard transition where the flux is the continuous function of the plasma radius and compare the structures of the potentials in the case of the soft and hard transitions. The hard-typed transition is accompanied by a spatial rapid change of the radial electric field when the multiple solutions of the ambipolar condition exist. On the other hand, the soft transition occurs with a spatial slow change of the radial electric field only one solution exists.

2. One-dimensional Model Equations

In this section, we show the model equations used here. We use the cylindrical coordinate and r-axis is

*Corresponding author's e-mail: toda@nifs.ac.jp

taken in the radial direction of the cylindrical plasma. We consider the region $0 \leq r \leq a$, where a is the minor radius. The expression for the radial neoclassical flux associated with helical-rippled trapped particle is given as [7]

$$\Gamma_j^{na} = -\varepsilon_i^2 \sqrt{\varepsilon_h} v_{dj}^2 n_j \int_0^\infty dx x^2 e^{-x} \tilde{v}_j \frac{A_j(x, E_r)}{\omega_j^2(x, E_r)}, \quad (1)$$

where $x \equiv m_j v^2 / (2T_j)$, $A_j(x, E_r) = n'_j / n_j - Z_j e E_r / T_j + (x - 3/2) T'_j / T_j$, $\omega_j^2(x, E_r) = 3 \tilde{v}_j^2(x) + 1.67 (\varepsilon_i / \varepsilon_h) (\omega_E + \omega_{Bj})^2 + (\varepsilon_i / \varepsilon_h)^{3/2} \omega_{Bj}^2 / 4 + 0.6 |\omega_{Bj}| \tilde{v}_j$ and $\tilde{v}_j(x) = v_{thj} / (\varepsilon_h x^{3/2})$. Here, the definitions $\omega_E = -E_r / (rB)$, $\omega_{Bj} = -T_j \varepsilon'_h x / (Z_j e r B)$ and $v_{dj} = -T_j / (Z_j e r B)$ are used. The quantities m_j , n_j , T_j , v_{thj} are the mass, the density, the temperature, the collision frequency using the thermal velocity for the species j and the parameters ε_i and ε_h are the toroidal and helical ripple, respectively. The prime denotes the derivative with respect to the radial direction. This expression for the particle flux is the connection formula and available for both the collisionless and collisional regimes. The energy flux related with neoclassical ripple transport is given as [7]

$$Q_j^{na} = q_j^{na} + \frac{5}{2} \Gamma_j^{na} T_i \\ = -\varepsilon_i^2 \sqrt{\varepsilon_h} v_{dj}^2 n_j T_j \int_0^\infty dx x^2 e^{-x} \tilde{v}_j(x) \frac{A_j(x, E_r)}{\omega_j^2(x, E_r)}. \quad (2)$$

The radial electric field equation in a nonaxisymmetric system is expressed by [9]

$$\frac{\partial E_r}{\partial t} = -\frac{e}{\varepsilon_\perp} \sum_j Z_j \Gamma_j^{na} \\ + \frac{1}{r} \frac{\partial}{\partial r} \left(\sum_j Z_j (D_{Ej} + D_{Ea}) r \frac{\partial E_r}{\partial r} \right), \quad (3)$$

where D_{Ea} is the anomalous component of the diffusion coefficient for the radial electric field and ε_\perp is the perpendicular dielectric coefficient as $\varepsilon_\perp = \varepsilon_0 ((c^2 / v_A^2) + 1) (1 + 2q^2)$. Here, ε_0 is the dielectric constant in the vacuum, c is the speed of light, v_A is the velocity of Alfvén wave and q is the safety factor. The factor $(1 + 2q^2)$ introduces the toroidal effect. [10] In Eq. (3), the neoclassical component of the diffusion coefficient is expressed by [9]

$$D_{Ej} = -\frac{e}{\varepsilon_\perp} \frac{3}{16\sqrt{2}\pi} \frac{Z_j e n_j v_{thj} T_j^4 \varepsilon_i^4}{T_j (Z_j e)^4 \sqrt{\varepsilon_h}} \\ \left(1 + \frac{\varepsilon_i}{\varepsilon_h} \right) \int_{x_p}^\infty \frac{dx e^{-x} x^3}{\left(|E_r| + \left| x \frac{T_j}{Z_j e} \varepsilon'_h \right| \right)^4}, \quad (4)$$

where $x_p = [v_{thj} / (\varepsilon_h (|E_r| + |T_j / (Z_j e) \varepsilon'_h|))]^{2/3}$. Both parameters D_{Ej} and D_a are used in the following analysis.

Equation (3) is solved together with the density and the temperature (ion and electron) equations. The equation for the density is

$$\frac{\partial n}{\partial t} = -\frac{1}{r} \frac{\partial}{\partial r} (r \Gamma^t) + S_n, \quad (5)$$

where Γ^t is the total particle flux written as $\Gamma^t = \Gamma^{an} - D_a \partial n / \partial r$. Here, D_a is the anomalous component of the particle diffusivity. The term S_n represents the particle source such as the ionization effect. The equation for the electron temperature is given as

$$\frac{3}{2} \frac{\partial}{\partial t} (n T_e) = -\frac{1}{r} \frac{\partial}{\partial r} (r Q_e^t) - \frac{m_e}{m_i} \frac{n}{\tau_e} (T_e - T_i) + P_{he}, \quad (6)$$

where Q_e^t is the total heat flux of the species j written as $Q_e^t = Q_e^{an} - n \chi_{aj} \partial T_j / \partial r$. Here, χ_{aj} is the anomalous part of the heat conductivity for the species j . The term τ_e denotes the electron collision time and the second term in the right hand side represents the heat exchange between ions and electrons. The parameter P_{he} represents the absorbed power due to the ECRH heating and its profile is assumed to be proportional to $\exp(-r / (0.2a)^2)$ for simplicity. The equation for the ion temperature is

$$\frac{3}{2} \frac{\partial}{\partial t} (n T_i) = -\frac{1}{r} \frac{\partial}{\partial r} (r Q_i^t) - \frac{m_e}{m_i} \frac{n}{\tau_e} (T_e - T_i) + P_{hi}. \quad (7)$$

The parameter P_{hi} represents the absorbed power of ions and its profile is also assumed to be proportional to $\exp(-r / (0.2a)^2)$.

3. Stationary Solutions with the Hard Transition

The density, temperature and electric field equations Eqs. (3), (5), (6) and (7) are solved under the appropriate boundary conditions. For the initial condition, we choose $E_r(r) \equiv 0$ and the plasma profiles evolve to the steady state. We fix the boundary condition at the center of plasma ($r = 0$) such as $\partial n / \partial r = \partial T_i / \partial r = \partial T_e / \partial r = E_r (= -\partial \phi / \partial r) = 0$, where ϕ is the electrostatic potential of the radial electric field. For the diffusion equation of the radial electric field Eq. (3), the boundary condition at the edge ($r = a$) is chosen as $\sum_j Z_j \Gamma_j = 0$. This implies that there is no momentum transport loss across the plasma surface. This simplified assumption is employed because the electric field bifurcation in the core plasma is the main subject of this

article. The boundary conditions at the edge ($r = a$) with respect to the density and the temperature are those expected in Compact Helical System (CHS): $-n/n' = 0.05$ m and $-T_e/T_e' = -T_i/T_i' = 0.02$ m. The machine parameters are those of the CHS device, such as the major radius $R = 1$ m, $a = 0.2$ m, toroidal mode number $m = 8$, poloidal mode number $l = 2$ and helical ripple $\epsilon_h(r) = lCI_l(mr/R)$, where I_l is the modified Bessel function of the first kind and the typical value of C is chosen according to the experimental condition. We consider the hydrogen plasma, so $Z_i = 1$ for the charge number in terms of ions. The particle source term S_n is assumed to be $S_n = S_0 \exp(100(r - a))$, where the value of S_0 is determined by the particle confinement time. Here, the value of S_0 is chosen as $S_0 = 10^{23}$ so as to study the case $\bar{n} \approx 10^{18} \text{ m}^{-3}$, where \bar{n} is the line-averaged density. For simplicity, the coefficient of the toroidal effect is chosen as $(1 + 2q^2) = 10$. The values for the anomalous parts of the diffusion coefficients are chosen as $D_a = 1 \text{ m}^2/\text{s}$, $\chi_{ae} = 5 \text{ m}^2/\text{s}$ and $\chi_{ai} = 1 \text{ m}^2/\text{s}$. The value of D_{Ea} is $D_{Ea} = 10 \text{ m}^2/\text{s}$. They do not necessarily coincide those in experiments. This simplification is employed to illustrate the existence of the electric field interface in CHS plasmas. These values are set to be constant spatially and temporally. In order to set the line-averaged temperature of electrons to be around $\bar{T}_e = 200$ eV, the absorbed power of electrons is around 10 kW, for this choice of χ_{ae} . The line-averaged ion temperature \bar{T}_i is chosen as about $\bar{T}_i = 400$ eV, where the absorbed power of ions is fixed as 6.25 kW. These values of the absorbed power are determined by the values of the anomalous diffusivities. The value of the absorbed power is different from the experimental condition because the anomalous diffusivities are set to be the smaller values compared with the observed values in experiments.

Using these parameters and the boundary conditions, we analyze Eqs. (3), (5), (6) and (7). The stationary solutions of the radial electric field are shown in Fig. 1 as the function of radial axis for the case of $\bar{T}_e = 130$ eV. Figure 2 shows the density profile (a) and the temperature profile of the ion and the electron (b). These profiles (E_r , n , T_e and T_i) are obtained from the calculation results of Eqs. (3), (5), (6) and (7). At the point $r = r_T$ (0.08 m), the transition characteristic is found. The positive solutions of the radial electric field correspond to the so-called electron roots and the negative solutions represent the ion roots, respectively. The circles in Fig. 1 show the values of the electric field which satisfy the ambipolar condition ($\Gamma_e^{na} = \Gamma_i^{na}$) for the

calculated profiles of the density and the temperatures. The multiple solutions are allowed from the ambipolar condition. At the transition point, the maximum value or the minimum value of the electric field shear is found to be taken. The transition points in the interface should be determined by the Maxwell construction. [10] The function $\Delta\Psi = \int_{E_1}^{E_2} (\Gamma_i^{na}(E_r) - \Gamma_e^{na}(E_r)) dE_r$ is introduced, where E_1 and E_2 are the stable solutions of the ambipolar condition. The relation $\Delta\Psi = 0$ represents the Maxwell construction. We confirm that the Maxwell construction is satisfied at the transition point in Fig. 1. The internal transport barrier is obtained for the channel of the neoclassical energy transport, being observed in both of the ion and electron temperature profiles in Fig. 2(b). In Fig. 3, the variations of the neoclassical part χ_j^{na} of the heat conductivity for the species j are shown. At the transition point, the rapid change of both of χ_e^{na} and χ_i^{na} is obtained. Within the radius of $r \leq r_T$, the transport barrier with reduced transport is formed. The steeper gradient is observed in the ion temperature profile than in the electron temperature profile in this case. This is caused by the choice of χ_{ja} values for the species j . The change of the density gradient at $r = r_T$ is also shown in Fig. 2(a).

Figure 4 shows the change of the regions of the electron root and the ion root when \bar{T}_e increases from 50 eV to 600 eV, by changing P_{he} . The absorbed power of ions is fixed at 6.25 kW and \bar{T}_i is around 400 eV. The term S_0 is set as $S_0 = 10^{23} \text{ m}^{-3} \text{ s}^{-1}$. When \bar{T}_e increases from 50 eV to 600 eV, the value of \bar{n} does not change and the change of \bar{T}_i is smaller than 40 eV. When the

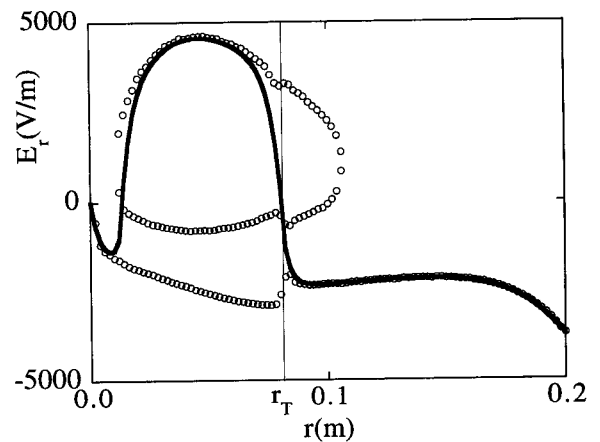


Fig. 1 Radial dependence of the electric field (Solid line). Circle marks show the electric field derived from the ambipolar condition.

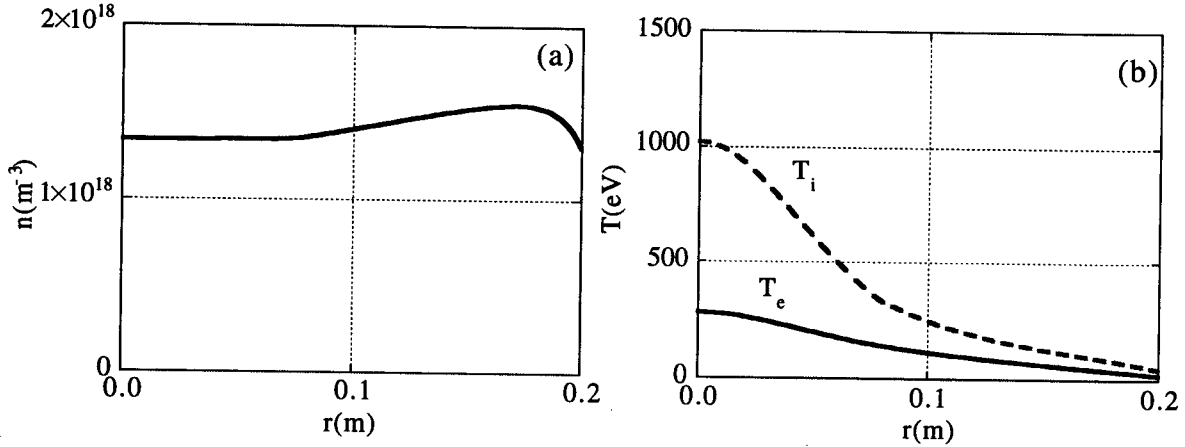


Fig. 2 Radial profile of the density (a) and the profiles of the temperature of ions and electrons (b) are shown. In Fig. 2(b), the dashed line represents the ion temperature and the solid line shows the electron temperature profile.

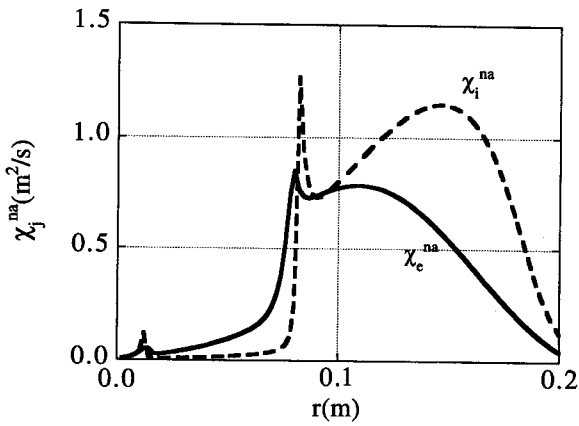


Fig. 3 Radial profiles of the neoclassical heat conductivity of electrons (solid line) and ions (dashed line) for the case of Fig. 2.

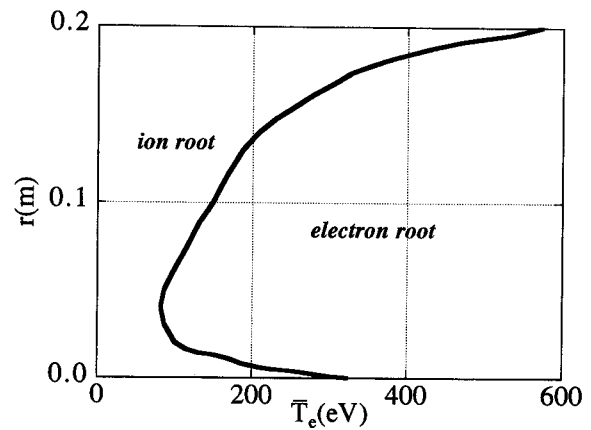


Fig. 4 Location of the domain interface as a function of \bar{T}_e . The change of the radial regions of the electron root and the ion roots when the line-averaged temperature of electron increases from 50 eV to 600 eV.

line-averaged temperature of electrons is low, all solutions are ion roots. On the other hand, all solutions become electron roots if \bar{T}_e increases up to 600 eV. The parameter regime ($80 \text{ eV} < \bar{T}_e < 600 \text{ eV}$) is found where the electron root exists in the inner region and the ion root exists in the outer region.

4. Hard and Soft Transitions

In experiments in CHS, the various types of potentials are observed. These potential are classified to many shapes, *e.g.*, bell-shape, dome-shape, hill-shape, Mexican hat-shape and well-shape. [8] In the previous section, we show the case where the hard transition in the potential profile takes place. In the case when \bar{T}_e is

80 eV, the shape of the potential looks like well-shape. When \bar{T}_e becomes 130 eV as is discussed in the previous section, the potential looks like Mexican hat-shape. The steep change of E_r , or the large E_r shear is obtained at $r = 0.08$ m, because the hard transition occurs at this point. The magnitude of the electric field shear is about $-5 \times 10^5 \text{ V/m}^2$ and enough large to reduce the fluctuations. Therefore the suppression of the anomalous transport diffusivities can be expected. If \bar{T}_e increases up to 600 eV, the potential shape looks like hill-shape. The absorbed power of ions is fixed at 6.25 kW and \bar{T}_i is around 400 eV. The term S_0 is set as $S_0 = 10^{23} \text{ m}^{-3} \text{ s}^{-1}$. If T_i is much lower than T_e , the multiple solutions are not

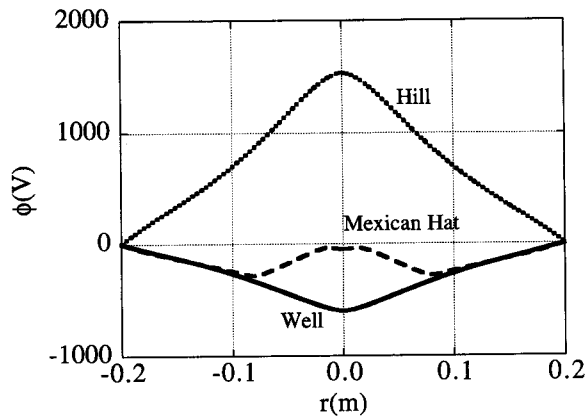


Fig. 5 Change of the potential profiles with the absorbed power. In the cases of the dotted (Hill), dashed (Mexican Hat), and solid (Well) lines, the line-averaged electron temperatures are 600 eV, 130 eV and 80 eV, respectively.

seen. Full description of the change between the hard and soft transition will be presented in a full paper. [11]

5. Summary and Discussions

In summary, the model equation of the radial electric field bifurcation is shown to contain the temporal and spatial evolutions of the plasma density, the temperatures and the radial electric field. The numerical formula of the non-axisymmetric components of neoclassical particle and heat fluxes in helical systems is included.

The stationary structure of the radial electric field in heliotron plasmas is examined and the hard-type transition with hysteresis characteristic is found. The state which corresponds to the internal transport barrier is obtained. It is found that the electron root and ion root co-exist. The states where the hard and soft transitions occur are obtained, depending on the ratio T_e/T_i . The

turbulence suppression due to the electric field shear -5×10^5 V/m² can be expected at the point where the hard transition occurs.

In this article, we set the anomalous diffusivities (D_a , χ_{aj} and D_{Ea}) to be constant, temporally and spatially. To compare the experimental results in details, the calculation by use of the turbulent model with respect to the anomalous diffusivities is needed. These are left for the future studies.

Acknowledgements

Authors would like to acknowledge Prof. S.-I. Itoh, Prof. A. Fukuyama, Dr. M. Yagi, Dr. A. Fujisawa and Dr. H. Sanuki for the useful discussions. This work is partly supported by Grant-in-Aid for Scientific Research on Ministry of Education, Science, Sports and Culture of Japan.

References

- [1] A. Fujisawa *et al.*, Phys. Rev. Lett. **79**, 1054 (1997).
- [2] A. Fujisawa *et al.*, Phys. Rev. Lett. **82**, 2669 (1999).
- [3] D.E. Hastings *et al.*, Nucl. Fusion **25**, 445 (1985).
- [4] K. Itoh *et al.*, *26th EPS Conf. on Control. Fusion and Plasma Phys.* Maastricht, The Netherlands 1309 (1999).
- [5] H. Sanuki *et al.*, J. Phys. Soc. Jpn. **69**, 445 (2000).
- [6] S. Toda *et al.*, J. Plasma Fusion Res. SERIES, Vol. 3 (2000), in press.
- [7] K.C. Shaing, Phys. Fluids **27**, 1567 (1984).
- [8] A. Fujisawa *et al.*, Phys. Plasmas **7**, 4152 (2000).
- [9] D.E. Hasting, Phys. Fluids **28**, 334 (1985).
- [10] K. Itoh, S.-I. Itoh and A. Fukuyama, *Transport and Structural Formation in Plasma* (IOP, 1999).
- [11] S. Toda and K. Itoh, Plasma Phys. Control. Fusion **43**, 629 (2001).